PHYSICAL REVIEW D VOLUME 5, NUMBER 9 1 MAY 1972

Model for the Pion-Pomeranchon Regge Cut in the Neutron-Proton Charge-Exchange Reaction*

Swee-Ping Chia
Department of Physics, University of Illinois at Urbana-Champaign, Urbana, Illinois 61801
(Received 26 October 1971)

A model is developed in which the pion-Pomeranchon Regge cut in the np charge-exchange reaction is calculated from the Mandelstam diagram. We find that the Regge cut is self-conspiratory, and is determined by two parameters besides those associated with the pion pole and the Pomeranchon. The sharp forward peak is reproduced through the destructive interference between the pole and the cut. An excellent fit is obtained in the small-t region, and the values of the parameters producing this fit agree with physical intuition.

I. INTRODUCTION

The np charge-exchange reaction[1-4] exhibits an exceptionally sharp forward peak with a width of $\Delta t \sim m_\pi^2$, followed by a more gradual exponential falloff. The shape of the differential cross section appears to be independent of energy. The sharp forward peak suggests that the reaction is probably controlled by pion exchange. However, an evasive pion gives rise to a forward dip. In order to reproduce the peak, a pure Regge-pole model necessitates that the pion conspire with a trajectory of opposite parity.[5-7] The fit is satisfactory provided a rapidly varying pion residue function with a zero at $-t \sim m_\pi^2$ is assumed. Among the objections to the conspirator-pole model are: (i) no particles are found to lie on the conspirator trajectory, (ii) a zero is present in the pion residue function in all π-exchanged reactions, (iii) it is incompatible with factorization. Using factorization alone, LeBellac[8] has shown that the reaction $\pi N \to \rho\Delta$ would have a forward dip if it were controlled by a conspiring pion. Experimental findings show quite the contrary[9,10]; a sharp forward peak is observed.

A more natural description of the data is possible if we consider, in addition to Regge poles, the contributions from Regge cuts. Phenomenological models[11-14] employing Regge cuts have been known to be successful. Theoretical ground for the presence of the Regge cuts is also overwhelming.[15-18] Regge cuts are present whenever two Regge poles are exchanged in the Mandelstam diagram.[15] Physically, we are primarily interested in the Regge cuts associated with the exchange of a Regge pole and a Pomeranchon. In this paper, we consider only the pion-Pomeranchon cut (πP cut).

Instead of generating the Regge cut through the process of rescattering or absorption, or through some kind of mathematical transform, we will generate our Regge cut through the Mandelstam diagram. We are further guided by the general requirement that the input ansatz for the pion-Pomeranchon Regge cut for a particular reaction must be the single-pion exchange to the same reaction. The simplest way to realize this requirement over a large class of reactions is to assume that the exchanged Pomeranchon is linked to the external particles through isoscalar scalar σ mesons. In the present case of the np charge-exchange reaction, we therefore picture the Mandelstam diagram as follows: The incoming nucleons emit σ mesons, which scatter via Pomeranchon exchange while the nucleons themselves scatter via pion exchange; the scattered σ mesons are subsequently reabsorbed by the outgoing nucleons, as shown in Fig. 1. We do not consider graphs in which the exchanged pion couples to the σ meson and the Pomeranchon to the nucleon, as these do not have the correct input ansatz. Moreover, the G parity is not right.

In Sec. II, the parametrization of both the on-shell and the off-shell π-pole amplitudes for NN scattering is discussed. The parametrization of the Pomeranchon amplitude for the $\sigma\sigma$ scattering is given in Sec. III. In Sec. IV, the calculation of the πP cut from the Mandelstam diagram is given. The πP-cut amplitudes are expressed in terms of the structure functions associated with the crosses. The explicit evaluation of the cross structure functions are given in Sec. V. Some qualitative features of the πP cut are discussed in Sec. VI. A fit of our model to the experimental data is given in Sec. VII, together with a discussion of the fit. An appendix is included to discuss the explicit forms of the form factors at the Regge vertex.

II. PARAMETRIZATION OF π-POLE AMPLITUDES

The on-shell π-pole amplitudes are assumed to be in the following form:

$$\mathfrak{F}^{(\pi)}_{\lambda_3\lambda_4;\lambda_1\lambda_2}(s,t)=C_\pi(t)\xi_\pi(t)\left(\frac{s}{s_0}\right)^{\varphi_\pi(t)}V^L_{\lambda_3\lambda_1}V^R_{\lambda_4\lambda_2}, \tag{2.1}$$

where $\varphi_\pi(t)$, $\xi_\pi(t)$, and $C_\pi(t)$ are the trajectory function, the signature factor, and the residue function, respectively, and V^L and V^R are the Reggeon vertex functions. The trajectory function is given by the usual expression

$$\varphi_\pi(t)=\varphi'_\pi(t-m_\pi{}^2),\quad \varphi'_\pi=1\ \text{GeV}^{-2}.$$

The signature factor is approximated at small t by

$$\xi_\pi(t)=\frac{e^{-i\pi\varphi_\pi(t)/2}}{\sin\frac{1}{2}\pi\varphi_\pi(t)}\simeq\frac{e^{-i\pi\varphi_\pi(t)/2}}{\frac{1}{2}\pi\varphi'_\pi(t-m_\pi{}^2)},$$

so as to display the pion pole explicitly. The residue function is assumed to be an exponential,

$$C_\pi(t)=Ce^{A_\pi t}.$$

The Reggeon vertex functions are taken to be the vertex functions for "bare" pion exchange,

$$V^L_{\lambda_3\lambda_1}=\bar{u}_{\lambda_3}(p_3)(-g_{pn\pi}\gamma_5)u_{\lambda_1}(p_1), \tag{2.2a}$$

$$V^R_{\lambda_4\lambda_2}=\bar{u}_{\lambda_4}(p_4)(-g_{pn\pi}\gamma_5)u_{\lambda_2}(p_2). \tag{2.2b}$$

The over-all strength C is determined by the known strength at the pion pole,[19] which gives

$$C=\tfrac{1}{2}\pi\varphi'_\pi e^{-A_\pi m_\pi{}^2}.$$

The on-shell π-pole amplitudes can then be rewritten as

$$\mathfrak{F}^{(\pi)}_{\lambda_3\lambda_4;\lambda_1\lambda_2}(s,t)=\frac{e^{A_\pi(t-m_\pi{}^2)}}{t-m_\pi{}^2}\left(e^{-i\pi/2}\frac{s}{s_0}\right)^{\varphi_\pi(t)}V^L_{\lambda_3\lambda_1}V^R_{\lambda_4\lambda_2}. \tag{2.3}$$

Expressed in this form, the on-shell amplitudes are determined by the parameter A_π, which shall be left as a free parameter.

We shall assume a similarly simple model for the off-shell π-pole amplitudes, effecting the continuation off shell by multiplying by form factors at the Reggeon vertices:

$$\mathfrak{F}^{(\pi)\text{off shell}}_{\lambda_3\lambda_4;\lambda_1\lambda_2}(p_3p_4;p_1p_2)=\mathfrak{F}^{(\pi)\text{on shell}}_{\lambda_3\lambda_4;\lambda_1\lambda_2}(s,t)G^L(p_1{}^2,p_3{}^2)G^R(p_2{}^2,p_4{}^2). \tag{2.4}$$

The form factors G^L and G^R must have the property that they become small when one of the external legs goes far off the mass shell, to ensure convergence of the integrals describing the πP cut. In the Appendix we discuss an explicit model for the pion-pole form factors in a general reaction. Here we shall merely quote the result relevant to our present case:

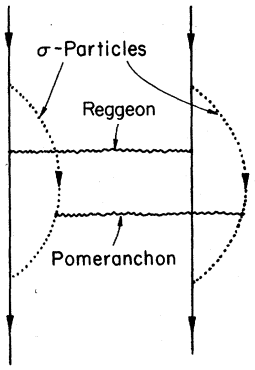

FIG. 1. Physical picture of the Mandelstam diagram. Incident nucleons emit σ particles, which scatter via Pomeranchon exchange while the nucleons scatter via pion exchange.

$$G^L(p_1{}^2,p_3{}^2)=\frac{m^2-\Lambda^2}{p_1{}^2-\Lambda^2+i\epsilon}\frac{m^2-\Lambda^2}{p_3{}^2-\Lambda^2+i\epsilon}, \tag{2.5a}$$

$$G^R(p_2{}^2,p_4{}^2)=\frac{m^2-\Lambda^2}{p_2{}^2-\Lambda^2+i\epsilon}\frac{m^2-\Lambda^2}{p_4{}^2-\Lambda^2+i\epsilon}. \tag{2.5b}$$

We shall assume that $\Lambda^2\gg m^2$. As we shall see later, the integrals describing the πP-cut amplitudes do not depend too sensitively on Λ^2, provided Λ^2 is sufficiently large. We may then let $\Lambda^2\to\infty$.

III. PARAMETRIZATION OF POMERANCHON AMPLITUDE

The Pomeranchon exchange is mediated through $\sigma\sigma$ scattering. Since this process cannot be measured, we again rely on the Regge-pole model. The trajectory function and the t dependence of the residue function are taken from elastic pp scattering. We find it unnecessary to assume form factors for the off-shell Pomeranchon amplitude, as the integrals described in Sec. IV converge without them. The amplitude is therefore given by

$$\mathfrak{F}^{(P)}(s,t)=-\gamma_P{}^2e^{A_Pt}\left(e^{-i\pi/2}\frac{s}{s_0}\right)^{\varphi_P(t)}. \tag{3.1}$$

In (3.1), we have approximated the signature factor by

$$\xi_P(t)\simeq e^{-i\pi\varphi_P(t)/2},\quad \varphi_P(t)=1+\varphi'_Pt.$$

The intercept of the Pomeranchon trajectory is taken to be unity. The slope of the trajectory and the slope of the residue function are, respectively,[20]

$$\varphi'_P=0.5\ \text{GeV}^{-2},\quad A_P=3.5\ \text{GeV}^{-2}. \tag{3.2}$$

A rough estimate for the dimensionless reduced residue $\gamma_P{}^2$ can be obtained. The optical theorem relates $\gamma_P{}^2$ to the total cross section,

$$\sigma_{\rm tot}^{(\sigma\sigma)} = \frac{1}{s}\,{\rm Im}\mathcal{F}^{(P)}(s,0) = \frac{1}{s_0}\gamma_P{}^2 .$$

If we further assume that

$$\sigma_{\rm tot}^{(\sigma\sigma)} \simeq \sigma_{\rm tot}^{(\pi\pi)} \simeq \tfrac{4}{9}\sigma_{\rm tot}^{(pp)} ,$$

we then have the estimate

$$\gamma_P{}^2 \simeq 45.6 . \qquad (3.3)$$

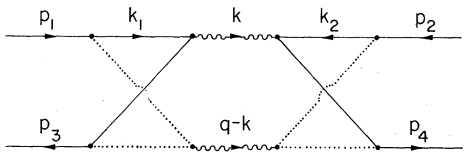

FIG. 2. Labeling of momenta for the Mandelstam diagram of Fig. 1.

IV. THE MANDELSTAM DIAGRAM

The s-channel helicity amplitudes corresponding to the Mandelstam diagram in Fig. 2 are

$$\mathcal{F}^{\rm cut}_{\lambda_3\lambda_4;\lambda_1\lambda_2} = i\int \frac{d^4k d^4k_1 d^4k_2}{(2\pi)^{12}}\left[\frac{e^{A_\pi(t_1-m_\pi{}^2)}}{t_1-m_\pi{}^2}\left(e^{-i\pi/2}\frac{s_1}{s_0}\right)^{\varphi_\pi(t_1)}\right]$$
$$\times\left[-\gamma_P{}^2 e^{A_P t_2}\left(e^{-i\pi/2}\frac{s_2}{s_0}\right)^{\varphi_P(t_2)}\right] G^L(k_1{}^2,(k_1-k)^2)G^R(k_2{}^2,(k_2+k)^2)X^L_{\lambda_3\lambda_1}X^R_{\lambda_4\lambda_2}, \qquad (4.1)$$

where $s_1=(k_1+k_2)^2$, $s_2=(p_1+p_2-k_1-k_2)^2$ are the squared subenergies of the internal Regge exchanges, and $t_1=k^2$, $t_2=(q-k)^2$ are the squared submomentum transfers. G^L and G^R are the Reggeon form factors given by (2.5a) and (2.5b); and X^L and X^R are

$$X^L_{\lambda_3\lambda_1} = \frac{\bar u_{\lambda_3}(ig_{\sigma NN})(\not k_1-\not k+m)(-g_{pn\pi}\gamma_5)(\not k_1+m)(ig_{\sigma NN})u_{\lambda_1}}{(k_1{}^2-m^2+i\epsilon)[(k_1-k)^2-m^2+i\epsilon][(p_1-k_1)^2-m_\sigma{}^2+i\epsilon][(p_1-q-k_1+k)^2-m_\sigma{}^2+i\epsilon]}, \qquad (4.2a)$$

$$X^R_{\lambda_4\lambda_2} = \frac{\bar u_{\lambda_4}(ig_{\sigma NN})(\not k_2+\not k+m)(-g_{pn\pi}\gamma_5)(\not k_2+m)(ig_{\sigma NN})u_{\lambda_2}}{(k_2{}^2-m^2+i\epsilon)[(k_2+k)^2-m^2+i\epsilon][(p_2-k_2)^2-m_\sigma{}^2+i\epsilon][(p_2+q-k_2-k)^2-m_\sigma{}^2+i\epsilon]} . \qquad (4.2b)$$

Instead of the set of 4-momentum components (k_0, k_x, k_y, k_z), we introduce, along the line of Gribov's approach,[18] a new set of variables $(\alpha, \beta, \vec{\rm k})$ defined by

$$\alpha = s^{-1/2}k_- = s^{-1/2}(k_0-k_z),$$
$$\beta = s^{-1/2}k_+ = s^{-1/2}(k_0+k_z), \qquad (4.3)$$
$$\vec{\rm k} = (k_x, k_y).$$

In terms of the new variables,

$$k^2 = \alpha\beta s - \vec{\rm k}^2,$$
$$\not k = \tfrac{1}{2}s^{1/2}\alpha\gamma_+ + \tfrac{1}{2}s^{1/2}\beta\gamma_- - \vec\gamma\cdot\vec{\rm k},$$
$$d^4k = \tfrac{1}{2}s\,d\alpha\,d\beta\,d^2\vec{\rm k}.$$

Turning to the integration, we invoke Gribov's finite-mass hypothesis[18] in order to extract the dominant region of integration. The assumption is that the internal Regge amplitudes are small if the invariant mass of one or more of the internal lines becomes large as fast as or faster than s. The dominant contribution therefore comes from a region where all internal invariant masses are finite. Further, we are interested only in the domain where both s_1 and s_2, the subenergies squared of the internal Regge amplitudes, are large, of order s.

The region of integration for the dominant contribution is easily evaluated from the preceding conditions. Written in terms of the new variables, this dominant region is given by the following set of equations:

$$\alpha,\ \alpha_1,\ \beta,\ \beta_2 \sim m^2/s;$$
$$\alpha_2,\ \beta_1 \sim 1;$$
$$\vec{\rm k}_1{}^2, \vec{\rm k}_2{}^2, \vec{\rm k}^2, (\vec{\rm k}_1-\vec{\rm k})^2, \ldots \sim m^2 .$$

The squares of the subenergies and the submomentum transfers are then given by $s_1=\alpha_2\beta_1 s$, $s_2=(1-\alpha_2)\times(1-\beta_1)s$, $t_1=-\vec{\rm k}^2=-\tau_1$, $t_2=-(\vec{\rm q}-\vec{\rm k})^2=-\tau_2$.

Expressing G^LX^L in terms of the new variables, and noting that $\beta\ll\beta_1$, we are able to show that G^LX^L is independent of β. Likewise we can show that G^RX^R is independent of α. The left-hand cross and the

right-hand cross are hence separated within the two-dimensional integration over $\vec{k}$, and we can cast $\mathcal{F}^{\rm cut}_{\lambda_3\lambda_4;\lambda_1\lambda_2}$ into the following form:

$$\mathcal{F}^{\rm cut}_{\lambda_3\lambda_4;\lambda_1\lambda_2}=\frac{1}{2s_0}\int\frac{d^2k}{(2\pi)^2}\frac{e^{-A_\pi(\tau_1+m_\pi{}^2)}}{\tau_1+m_\pi{}^2}e^{-A_P\tau_2}\left(e^{-i\pi/2}\frac{s}{s_0}\right)^{\varphi_\pi(\tau_1)+\varphi_P(\tau_2)-1}N^L_{\lambda_3\lambda_1}N^R_{\lambda_4\lambda_2}, \tag{4.4}$$

where we have put all the integrations over the internal variables of the left-hand cross in $N^L_{\lambda_3\lambda_1}$, and those of the right-hand in $N^R_{\lambda_4\lambda_2}$. We shall refer to $N^L_{\lambda_3\lambda_1}$ and $N^R_{\lambda_4\lambda_2}$ as the cross structure functions. The explicit expressions for the cross structure functions are

$$\begin{aligned}N^L_{\lambda_3\lambda_1}=&-s^2\frac{g_{\sigma NN}{}^2}{4\pi}g_{p n\pi+\gamma_P}\int\frac{d^2k_1\,d\alpha_1\,d\beta_1\,d\alpha}{(2\pi)^4}\beta_1{}^{\varphi_\pi(\tau_1)}(1-\beta_1)^{\varphi_P(\tau_2)}\\&\times\frac{m^2-\Lambda^2}{\alpha_1\beta_1 s-\vec{k}_1{}^2-\Lambda^2+i\epsilon}\,\frac{m^2-\Lambda^2}{(\alpha_1-\alpha)\beta_1 s-(\vec{k}_1-\vec{k})^2-\Lambda^2+i\epsilon}\\&\times\frac{\bar{u}_{\lambda_3}\left[\frac{1}{2}s^{1/2}(\alpha_1-\alpha)\gamma_+ +\frac{1}{2}s^{1/2}\beta_1\gamma_- -\vec{\gamma}\cdot(\vec{k}_1-\vec{k})+m\right]\gamma_5}{\left[(\alpha_1-\alpha)\beta_1 s-(\vec{k}_1-\vec{k})^2-m^2+i\epsilon\right]\left\{\left[\alpha_1-\alpha-(m^2+\tau)/s\right](\beta_1-1)s-(\vec{k}_1-\vec{k}+\vec{q})^2-m_\sigma{}^2+i\epsilon\right\}}\\&\times\frac{(\frac{1}{2}s^{1/2}\alpha_1\gamma_+ +\frac{1}{2}s^{1/2}\beta_1\gamma_- -\vec{\gamma}\cdot\vec{k}_1+m)u_{\lambda_1}}{(\alpha_1\beta_1 s-\vec{k}_1{}^2-m^2+i\epsilon)\left[(\alpha_1-m^2/s)(\beta_1-1)s-\vec{k}_1{}^2-m_\sigma{}^2+i\epsilon\right]},\end{aligned} \tag{4.5}$$

and a similar expression for $N^R_{\lambda_4\lambda_2}$.

V. THE CROSS STRUCTURE FUNCTIONS

The cross structure functions can be interpreted as the production amplitudes of the Reggeons, corresponding to the diagram of Fig. 3. We shall later see that, as expressed in (4.5), they are independent of s in the limit of large s. We shall also establish a symmetry between the left- and the right-hand crosses.

For the left-hand cross, we note that when we make the following change of integration variables in (4.5);

$$\int\int d\alpha_1 d\alpha\to\int\int d\alpha_1 d(\alpha_1-\alpha),$$

the integrand then breaks up into two parts, one involving only α_1 integration and the other only $(\alpha_1-\alpha)$ integration. The α_1 integration part consists of the expression

$$T=\int_{-\infty}^{\infty}\frac{d\alpha_1}{2\pi}\frac{m^2-\Lambda^2}{\alpha_1\beta_1 s-\vec{k}_1{}^2-\Lambda^2+i\epsilon}\,\frac{\frac{1}{2}s^{1/2}\alpha_1\gamma_+ +\frac{1}{2}s^{1/2}\beta_1\gamma_- -\vec{\gamma}\cdot\vec{k}_1+m}{\alpha_1\beta_1 s-\vec{k}_1{}^2-m^2+i\epsilon}\,\frac{1}{(\alpha_1-m^2/s)(\beta_1-1)s-\vec{k}_1{}^2-m_\sigma{}^2+i\epsilon}. \tag{5.1}$$

The integrand of (5.1) contains three denominators: one coming from the propagator of the nucleon line (1) of Fig. 3, one from the propagator of the σ line (3), and the third from the form factor associated with the nucleon line (1). It is worth noting that the third denominator is necessary to make (5.1) convergent.

Treating (5.1) as a contour integral, we note that it vanishes whenever all three poles are displaced onto the same side of the real axis in the complex α_1 plane. To prevent (5.1) from vanishing, we want one of the poles to be on the opposite side of the real axis from the other two poles. This can be achieved only if β_1 is confined between the values of 0 and 1,

$$0<\beta_1<1. \tag{5.2}$$

When the condition is satisfied, the σ pole is in the upper half-plane, whereas the other two are in the lower half-plane. We can then close the contour in the upper half-plane and pick up the contribution from the σ pole. Equivalently we replace the σ propagator by a δ function,

$$\left[(\alpha_1-m^2/s)(\beta_1-1)s-\vec{k}_1{}^2-m_\sigma{}^2+i\epsilon\right]^{-1}=\frac{-2\pi i}{(1-\beta_1)s}\delta\left(\alpha_1-\frac{m^2}{s}+\frac{\vec{k}_1{}^2+m_\sigma{}^2}{(1-\beta_1)s}\right). \tag{5.3}$$

The evaluation of the $(\alpha_1-\alpha)$ integration is identical, and we obtain

$$\left\{\left[\alpha_1-\alpha-(m^2+\tau)/s\right](\beta_1-1)s-(\vec{k}_1-\vec{k}+\vec{q})^2-m_\sigma{}^2+i\epsilon\right\}^{-1}=\frac{-2\pi i}{(1-\beta_1)s}\delta\left(\alpha_1-\alpha-\frac{m^2+\tau}{s}+\frac{(\vec{k}_1-\vec{k}+\vec{q})^2+m_\sigma{}^2}{(1-\beta_1)s}\right). \tag{5.4}$$

Having performed the α_1 and $(\alpha_1 - \alpha)$ integrations in (4.5), we next approximate by letting $\Lambda^2 \to \infty$. This will effectively remove two of the four denominators remaining in (4.5), thus greatly simplifying the evaluation of the cross structure functions. Justification for making such an assumption lies in the fact that the cross structure functions are not too sensitive to the particular values of Λ^2, provided Λ^2 is sufficiently large.[21] The assumption has the further advantage that our final expressions for the cut amplitudes have one less free parameter.

Letting $\Lambda^2 \to \infty$, and combining the two remaining denominators, we obtain

$$N^L_{\lambda_3\lambda_1} = \frac{g_{\sigma NN}{}^2}{4\pi} g_{pn\pi+\gamma P} \int_0^1 d\beta_1 \beta_1{}^{\varphi_\pi(\tau_1)}(1-\beta_1)^{\varphi_P(\tau_2)} \int_0^1 dx \int \frac{d^2k_1'}{(2\pi)^2} \frac{B^L_{\lambda_3\lambda_1}}{[\vec{k}_1'^2 + x(1-x)(\vec{k}-\beta_1\vec{q})^2 + (1-\beta_1)^2 m^2 + \beta_1 m_\sigma{}^2 - i\epsilon]^2}, \tag{5.5}$$

where $\vec{k}_1' = \vec{k}_1 - x(\vec{k} - \beta_1\vec{q})$, and $B^L_{\lambda_3\lambda_1}$, the cross numerator functions, are

$$B^L_{\lambda_3\lambda_1} = \bar{u}_{\lambda_3}[\tfrac{1}{2}s^{1/2}(\alpha_1 - \alpha)\gamma_+ + \tfrac{1}{2}s^{1/2}\beta_1\gamma_- - \vec{\gamma}\cdot(\vec{k}_1 - \vec{k}) + m]\gamma_5[\tfrac{1}{2}s^{1/2}\alpha_1\gamma_+ + \tfrac{1}{2}s^{1/2}\beta_1\gamma_- - \vec{\gamma}\cdot\vec{k}_1 + m]u_{\lambda_1}. \tag{5.6}$$

The evaluation of the cross numerator functions for the various helicity states is straightforward but tedious. We shall omit the details and show the results directly. We find that the $B^L_{\lambda_3\lambda_1}$ obey the following relation:

$$B^L_{\lambda_3\lambda_1} = (-1)^{\lambda_3+\lambda_1} B^{L*}_{-\lambda_3,-\lambda_1}, \tag{5.7}$$

so that it is only necessary to calculate B^L_{++} and B^L_{+-}. Explicitly, they are

$$\begin{aligned}
&\mathrm{Re}B^L_{++} = -\frac{1}{2}\frac{1+\beta_1}{1-\beta_1}(1-2x)(\vec{k}-\vec{q})\cdot(\vec{k}-\beta_1\vec{q}),\\
&\mathrm{Im}B^L_{++} = \tfrac{1}{2}(1+\beta_1)\tau^{1/2}k_y,\\
&\mathrm{Re}B^L_{+-} = \frac{k_x}{2m}\frac{1}{1-\beta_1}\{(3+\beta_1)(1-\beta_1)m^2 - m_\sigma{}^2 - x(1-x)[\vec{k}^2 - 2\vec{k}\cdot\vec{q} + \beta_1(2+\beta_1)\vec{q}^2]\}\\
&\qquad - \frac{\tau^{1/2}}{2m}\frac{1}{1-\beta_1}\{(1-\beta_1)^2m^2 + \beta_1 m_\sigma{}^2 - x(1-x)[(1-2\beta_1)\vec{k}^2 + \beta_1{}^2\vec{q}^2]\},\\
&\mathrm{Im}B^L_{+-} = -\frac{k_y}{2m}\frac{1}{1-\beta_1}\{(3+\beta_1)(1-\beta_1)m^2 - m_\sigma{}^2 - x(1-x)[\vec{k}^2 - 2\vec{k}\cdot\vec{q} + \beta_1(2-\beta_1)\vec{q}^2] - \tfrac{1}{2}\beta_1{}^2\vec{q}^2\}.
\end{aligned} \tag{5.8}$$

Because the x integral is symmetric about the point $x = \frac{1}{2}$, and $\mathrm{Re}B^L_{++}$ is antisymmetric about this point, there will be no contribution from $\mathrm{Re}B^L_{++}$ in our answer. The $\vec{k}_1'$ integration in (5.5) is trivially performed, giving

$$N^L_{\lambda_3\lambda_1} = \frac{g_{\sigma NN}{}^2}{4\pi}\frac{g_{pn\pi+\gamma P}}{4\pi}\int_0^1 d\beta_1\beta_1{}^{\varphi_\pi(\tau_1)}(1-\beta_1)^{\varphi_P(\tau_2)}\int_0^1 dx \frac{B^L_{\lambda_3\lambda_1}}{(1-\beta_1)^2m^2 + \beta_1 m_\sigma{}^2 + x(1-x)(\vec{k}-\beta_1\vec{q})^2}. \tag{5.9}$$

From (5.8) and (5.9), it is obvious that $N^L_{\lambda_3\lambda_1}$ does not depend on s, and the energy dependence of the amplitudes is given by (4.4), which clearly exhibits Regge-cut behavior.

The calculation of the right-hand cross is identical to that of the left-hand cross. In analogy to the spinless case, a left-right symmetry is displayed by the structure functions,

$$N^R_{\lambda,\mu} = -N^L_{-\lambda,-\mu}. \tag{5.10}$$

Supplementing (5.10) is the relation (5.7), which, when stated in terms of the structure functions, reads

$$N^{R,L}_{\lambda,\mu} = (-1)^{\lambda+\mu}N^{R,L*}_{-\lambda,-\mu}. \tag{5.11}$$

We can further simplify (5.9) by carrying out the x integrations analytically, which gives

$$N^L_{\lambda_3\lambda_1} = \frac{g_{\sigma NN}{}^2}{4\pi}\frac{g_{pn\pi+\gamma P}}{4\pi}\int_0^1 d\beta_1\beta_1{}^{\varphi_\pi(\tau_1)}(1-\beta_1)^{\varphi_P(\tau_1)-1}D^L_{\lambda_3\lambda_1}. \tag{5.12}$$

The functions $D^L_{\lambda_3\lambda_1}$ are defined by

$$\begin{aligned}
&\mathrm{Re}D^L_{++} = 0,\\
&\mathrm{Im}D^L_{++} = \frac{\tau^{1/2}\tau_1{}^{1/2}}{4m^2}\sin\varphi(1-\beta_1{}^2)K(\rho,\omega),
\end{aligned}$$

$$\mathrm{Re}D^L_{+-} = -\frac{\tau_1^{1/2}}{2m}\cos\varphi\left[\tfrac{1}{2}(1-\beta_1)\eta K(\rho,\omega)+1\right] - \frac{\tau^{1/2}}{2m}\left[\rho K(\rho,\omega)-1\right] \tag{5.13}$$

$$-\frac{\tau_1^{1/2}\tau^{1/2}}{2m^2}\left(\frac{\tau_1^{1/2}}{2m}(\cos^2\varphi+\beta_1\sin^2\varphi)+\frac{\tau^{1/2}}{2m}\cos\varphi(1+\beta_1)\right)L(\rho,\omega),$$

$$\mathrm{Im}D^L_{+-} = \frac{\tau_1^{1/2}}{2m}\sin\varphi\left[\left[\tfrac{1}{2}(1-\beta_1)\eta K(\rho,\omega)+1\right]+\beta_1^{\,2}\frac{\tau}{4m^2}K(\rho,\omega)+2(1-\beta_1)\frac{\tau^{1/2}}{2m}\left(\frac{\tau_1^{1/2}}{2m}\cos\varphi+\beta_1\frac{\tau^{1/2}}{2m}\right)L(\rho,\omega)\right],$$

where we have defined,

$$K(\rho,\omega)=\frac{1}{\omega}\left(\frac{\omega}{\rho+\omega}\right)^{1/2}\ln\left(\frac{1+[\omega/(\rho+\omega)]^{1/2}}{1-[\omega/(\rho+\omega)]^{1/2}}\right),$$

$$L(\rho,\omega)=\frac{1}{\omega}[1-\tfrac{1}{2}\rho K(\rho,\omega)].$$

The quantities ρ, ω, and η are defined by

$$\rho=(1+\beta_1)^2+\beta_1\eta,$$

$$\omega=\frac{1}{4m^2}(\vec{k}-\beta_1\vec{q})^2$$

$$=\frac{1}{4m^2}(\tau_1+\beta_1^{\,2}\tau+2\beta_1\tau^{1/2}\tau_1^{1/2}\cos\varphi),$$

$$\eta=\frac{m_\sigma^{\,2}}{m^2}-4.$$

The angle φ is introduced such that $k_x=\tau_1^{1/2}\cos\varphi$, $k_y=\tau_1^{1/2}\sin\varphi$, $\tau_2=\tau+\tau_1+2\tau^{1/2}\tau_1^{1/2}\cos\varphi$ and $d^2k=\frac{1}{2}d\tau_1 d\varphi$.

Let us take a closer look at $N^L_{\lambda_3\lambda_1}$ in (5.12). The functions $D^L_{\lambda_3\lambda_1}$ as given in (5.13) are well behaved in β_1. Hence the behavior of $N^L_{\lambda_3\lambda_1}$ depends on the behavior of the expression

$$\beta_1^{\,\varphi_\pi(\tau_1)}(1-\beta_1)^{\varphi_P(\tau_2)-1}. \tag{5.14}$$

We know that the integral $\int_0^1 d\beta_1\beta_1^{\,a}(1-\beta_1)^b$ diverges for $a<-1$, or $b<-1$, due to the singularity of the integrand at the end points $\beta_1=0$ and $\beta_1=1$. It follows that $N^L_{\lambda_3\lambda_1}$ diverges if $\varphi_\pi(\tau_1)<-1$ or $\varphi_P(\tau_2)<0$. These correspond to

$$\tau_1>\frac{1}{\varphi'_\pi}-m_\pi^{\,2}\sim 1\,\mathrm{GeV}^2 \quad \text{or} \quad \tau_2>\frac{1}{\varphi'_P}\sim 2\,\mathrm{GeV}^2.$$

It thus appears that the structure functions break down at sufficiently large values of τ_1, even though τ is small.

However, this is not necessarily the case. Since the divergence comes from the end-point contributions, we intuitively suspect that the physics that we put in at the end points may not be correct. The lower end point $\beta_1\to 0$ corresponds to $s_1\sim m^2$, and the upper end point $\beta_1\to 1$ corresponds to $s_2\sim m^2$. Clearly, at these end points, the internal amplitudes are non-Regge-like. Hence the Regge amplitudes (2.3) and (3.1) do not represent the true internal amplitudes correctly at the end points of the β_1 integration. To avoid this difficulty, we have to use the correct low-energy amplitudes at the end points. This will certainly make the calculation too complicated. Instead, we shall simply replace the expression of (5.14) by the value at midpoint,[17]

$$\beta_1^{\,\varphi_\pi(\tau_1)}(1-\beta_1)^{\varphi_P(\tau_2)-1}\to\left(\tfrac{1}{2}\right)^{\varphi_\pi(\tau_1)+\varphi_P(\tau_2)-1}. \tag{5.15}$$

For small values of τ_1 and τ_2, the replacement (5.15) appears to be a good approximation. A possible error of less than 5% is estimated for values of τ_1 and τ_2 less than 0.2 GeV^2. This approximation has the further advantage that the integrations in (5.12) are easily performed numerically. Since the integrands do not have any singularities along the contour of integration, the real and imaginary parts of the cross structure functions are therefore real analytic.

VI. THE πP-CUT AMPLITUDES

In the preceding sections, we have employed the Mandelstam diagram as the generator of a πP cut in the np charge-exchange reaction, and we have arrived at the expressions given in (4.4), (5.12), and (5.13). In this section, a few qualitative features of the cut will be discussed. We find it more natural to define the following linear combinations of s-channel helicity amplitudes:

$$\begin{aligned} h_1&=\mathcal{F}_{++;++}+\mathcal{F}_{+-;+-},\\ h_2&=\mathcal{F}_{++;++}-\mathcal{F}_{+-;+-},\\ h_3&=\mathcal{F}_{++;--}+\mathcal{F}_{+-;-+},\\ h_4&=\mathcal{F}_{++;--}-\mathcal{F}_{+-;-+},\\ h_5&=\mathcal{F}_{++;+-}. \end{aligned} \tag{6.1}$$

The πP-cut contributions to these amplitudes can be cast into the following form:

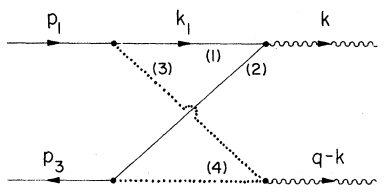

FIG. 3. Section of the diagram represented by a cross structure function.

$$h_i^{\rm cut}(s,\tau)=\frac{C_f}{8\pi^2 s_0}\int_0^\infty d\tau_1\int_0^{2\pi}d\varphi\,\frac{e^{-A_\pi(\tau_1+m_\pi^2)}}{\tau_1+m_\pi^2}\times e^{-A_P\tau_2}\left(e^{-i\pi/2}\frac{s}{s_0}\right)^{\varphi_\pi+\varphi_P-1}\mathcal{K}_i\,, \tag{6.2}$$

where

$$C_f=\left(\frac{g_{\sigma NN}^{\ 2}}{4\pi}\right)^2\frac{g_{pn\pi^+}^{\ 2}}{8\pi}\,\frac{\gamma_P^{\ 2}}{4\pi} \tag{6.3}$$

and

$$\begin{aligned}
\mathcal{K}_1&=2\left(\int_0^1 d\beta_1\beta_1^{\varphi_\pi}(1-\beta_1)^{\varphi_P-1}\,\mathrm{Im}D^L_{++}\right)^2,\\
\mathcal{K}_2&=0,\\
\mathcal{K}_3&=-2\left(\int_0^1 d\beta_1\beta_1^{\varphi_\pi}(1-\beta_1)^{\varphi_P-1}\,\mathrm{Re}D^L_{+-}\right)^2,\\
\mathcal{K}_4&=-2\left(\int_0^1 d\beta_1\beta_1^{\varphi_\pi}(1-\beta_1)^{\varphi_P-1}\,\mathrm{Im}D^L_{+-}\right)^2,\\
\mathcal{K}_5&=-\left(\int_0^1 d\beta_1\beta_1^{\varphi_\pi}(1-\beta_1)^{\varphi_P-1}\,\mathrm{Im}D^L_{++}\right)\\
&\quad\times\left(\int_0^1 d\beta_1\beta_1^{\varphi_\pi}(1-\beta_1)^{\varphi_P-1}\,\mathrm{Im}D^L_{+-}\right).
\end{aligned} \tag{6.4}$$

In writing down (6.4), we have made explicit use of the relations (5.10) and (5.11), and the fact that in (5.13) the real part of $D^L_{\lambda\mu}$ is even in φ whereas the imaginary part is odd, so that crossed terms like $(\mathrm{Re}D^L_{\lambda_3\lambda_1}\mathrm{Im}D^R_{\lambda_4\lambda_2})$ do not contribute.

The πP cut, whose contributions to the s-channel amplitudes are given in (6.2) and (6.4), is readily shown to be self-conspiratory, which means that it contributes to the t-channel parity-conserving helicity amplitudes of both parities. The conspiracy relation, as we recall, relates parity-conserving helicity amplitudes of opposite parities. Translated into the s-channel amplitudes of (6.1), the conspiracy relation reads

$$h_3(s,0)-h_4(s,0)=0. \tag{6.5}$$

The amplitude h_3 comes from purely unnatural-parity amplitudes, whereas h_4 receives a major contribution from the natural-parity amplitudes. It is obvious from (6.4) and (5.13) that, in the forward direction,

$$\mathcal{K}_1=\mathcal{K}_2=\mathcal{K}_5=0$$

and

$$\mathcal{K}_3=\mathcal{K}_4\neq 0,$$

so that

$$h_3^{\rm cut}(s,0)=h_4^{\rm cut}(s,0)\neq 0,$$

and the conspiracy relation (6.5) is satisfied non-trivially. Hence the πP cut is self-conspiratory.

Although the πP cut does not have a fixed parity, it nevertheless has definite signature and isospin. The isospin of the cut is just the isospin of the π pole, since the Pomeranchon does not carry an isospin. The signature of the cut is the product of the signatures of the π pole and the Pomeranchon.[22] Since both the π pole and the Pomeranchon have even signature, the resulting signature of the cut must be even. This is readily seen by explicitly calculating the contribution of the πP cut to the line-reversed reaction, $\bar{p}p\to\bar{n}n$; we find that

$$\mathcal{F}^{\rm cut}(np\to pn)=\mathcal{F}^{\rm cut}(\bar{p}p\to\bar{n}n),$$

which confirms that the signature is, indeed, even.

The s and t dependence of the πP-cut amplitudes can be roughly estimated as follows:

$$\begin{aligned}
h_i^{\rm cut}&\sim\int d\tau_1 d\varphi\, e^{-A_\pi\tau_1}e^{-A_P\tau_2}\left(\frac{s}{s_0}\right)^{\varphi_\pi(\tau_1)+\varphi_P(\tau_2)-1}\\
&\sim\frac{1}{\ln(s/s_0)}\left(\frac{s}{s_0}\right)^{\varphi_c(\tau)}e^{-A_c\tau},
\end{aligned}$$

where

$$\varphi_c(\tau)=\varphi_\pi(0)+\varphi_P(0)-1+\frac{\varphi'_\pi\varphi'_P}{\varphi'_\pi+\varphi'_P}\tau$$

and

$$A_c=\frac{\varphi'^2_\pi A_P+\varphi'^2_P A_\pi}{(\varphi'_\pi+\varphi'_P)^2}\,.$$

For $A_P=3.5$ GeV^{-2} and $A_\pi=4.7$ GeV^{-2} (taken from the fit described in Sec. VII), we obtain $A_c\simeq 2$ GeV^{-2}. The πP cut is therefore considerably flatter than the π pole.

The mechanism through which a flat and self-conspiratory πP cut can account for the sharp forward peak is by means of destructive interference with the π pole.[11] To see that the πP cut chooses, indeed, this particular mechanism, we note that the π pole contributes only to h_3, which is, from (2.3) and (2.4),

$$h_3^{(\pi)}=\frac{g_{pn\pi^+}^{\ 2}}{2m^2}\,\frac{\tau}{\tau+m_\pi^{\ 2}}e^{-A_\pi(\tau+m_\pi^2)}\left(e^{-i\pi/2}\frac{s}{s_0}\right)^{\varphi_\pi(\tau)}. \tag{6.6}$$

The contribution of the πP cut to h_3, however, is

$$h_3^{\rm cut}=-\frac{C_f}{4\pi^2 s_0}\int_0^\infty d\tau_1\int_0^{2\pi}d\varphi\,\frac{e^{-A_\pi(\tau_1+m_\pi^2)}}{\tau_1+m_\pi^2}e^{-A_P\tau_2}\left(e^{-i\pi/2}\frac{s}{s_0}\right)^{\varphi_\pi+\varphi_P-1}\left(\int_0^1 d\beta_1\beta_1^{\varphi_\pi}(1-\beta_1)^{\varphi_P-1}\,\mathrm{Re}D^L_{+-}\right)^2. \tag{6.7}$$

It is obvious that h_3^{cut} is almost completely out of phase with $h_3^{(\pi)}$. The destructive interference is clearly illustrated in Fig. 4.

We note also that the πP-cut contribution to h_2 is absent. We can show that h_2, when crossed into the t channel, is predominantly A_1-like, i.e., it has quantum number $P=C=-(-1)^J$. Our model therefore predicts that the πP cut in the np charge-exchange reaction does not have an A_1-like contribution. This agrees with the product rule for the signature of the Regge cut.

As given in (6.1), (6.3), and (5.13), the πP-cut amplitudes are expressed in terms of three parameters, A_π, C_f, and η. The parameter A_π is the slope of the π-pole residue function, and C_f and η are related to more fundamental quantities, namely, the σ-nucleon coupling constant and the mass of the σ particle, respectively.

VII. DESCRIPTION OF THE FIT

The differential cross section is calculated from the following formula:

$$\frac{d\sigma}{dt}=\frac{m^4}{4\pi s(s-4m^2)}(|h_1|^2+|h_2|^2+|h_3|^2+|h_4|^2+8|h_5|^2), \tag{7.1}$$

where the total amplitudes h_i are given by

$$h_i=h_i^{(\pi)}+h_i^{\text{cut}}.$$

The cross section, as given in (7.1), contains three free parameters.

Recent experiments on the np charge-exchange reaction are reported by Miller *et al.*[3] and Engler *et al.*,[4] providing us with an abundance of data. However, since we do not include the contributions of other Regge poles, such as ρ and A_2, an elaborate fit utilizing all the data points is not necessary. We therefore employ only a small portion of the data – the 10-GeV/c data of Miller *et al.* Only the first 23 points are used for our fit, corresponding to a range of t up to $t=-0.105$ GeV^2. The choice of the small-t cross section for our fit stems from the belief that at higher values of t, other Regge exchanges may become important.

The fit is shown in Fig. 5; the corresponding χ^2 value is 2.0. This is excellent, considering the small number of free parameters. One feature is worth noting, i.e., the theoretical curve is void of any structure whereas the data appears to exhibit a slight structure at $t=-0.03$ GeV^2. The structure, however, may or may not be significant. From the fit, the following values are obtained for the three parameters: $A_\pi=4.7$ GeV^{-2}, $C_f=1.17\times10^4$, and $\eta=10$. The corresponding values for the parameters associated with the σ particle are, $g_{\sigma NN}^2/4\pi=14.7$ and $m_\sigma=3.52$ GeV. The σ-nucleon coupling constant has the right strength, compared with a value of 15 for the pion-nucleon coupling constant. The mass of the σ particle is also the right order of magnitude.

From the fit, we observe that the πP cut contributes significantly only to h_3 and h_4, the two amplitudes involved in the conspiracy relation. Although the cut contributes also to h_1 and h_5, these contributions are strongly suppressed. The cut amplitudes can be approximated by the following form:

$$h_i^{\text{cut}}\simeq\gamma_{ci}(\tau)e^{-i\pi[\varphi_c(\tau)-\lambda_c]/2}\frac{(s/s_0)^{\varphi_c(\tau)}}{\ln(s/s_0)},$$

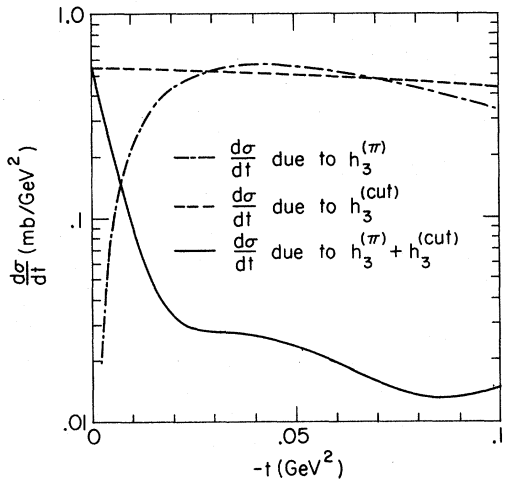

FIG. 4. Illustration of pole-cut destructive interference.

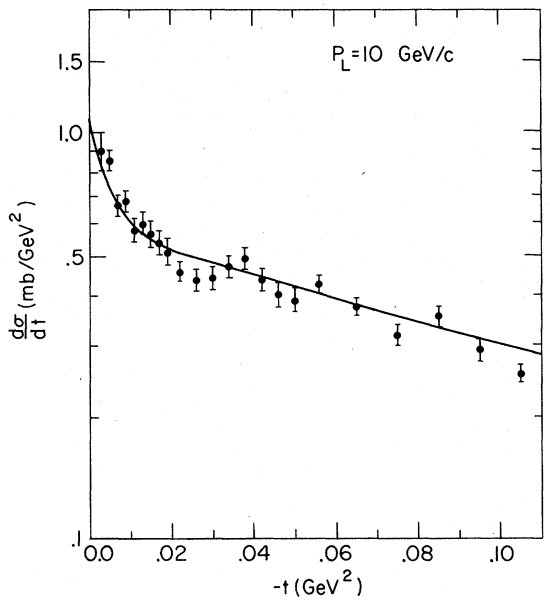

FIG. 5. Fit of the model to data of Miller *et al.*, Ref. 3. Parameters in the model are adjusted to fit this data sample only.

where $\varphi_c(\tau)$ is the trajectory function of the cut, and is given by

$$\varphi_c(\tau) = \varphi_\pi(0) + \varphi_P(0) - 1 - \frac{\varphi'_\pi \varphi'_P}{\varphi'_\pi + \varphi'_P}\tau$$

$$= -0.02 - 0.33\tau .$$

λ_c is an extra phase acquired by the cut amplitudes, which is

$$\lambda_c = 0.17.$$

The presence of this extra phase is a surprising feature of our model; it suggests that the phase of the cut amplitudes is not determined solely by the signature factor, which is $e^{-i\pi\varphi_c(\tau)/2}$. Equally surprising is that we have only one λ_c for the different amplitudes. Absorbing this extra phase into the cut "residue function," we are led to infer that the complex cut "residue functions" have a common phase although they have widely varied magnitudes.

A list of the cut "residue functions" $\gamma_{ci}(\tau)$ is given in Table I, in which the relative strengths of the cut amplitudes are displayed. It is readily observed that h_1^{cut} and h_5^{cut} are smaller than h_3^{cut} and h_4^{cut} by a factor of 10^{-2}; in addition, they are further suppressed at small t by the respective kinematic factors, τ and $\tau^{1/2}$.

At larger values of t, the theoretical curve exhibits a distinctive shoulder around $t = -0.3$ GeV^2, which is shown in comparison with the data of Ref. 3 in Fig. 6. The data, on the contrary, is quite smooth. Although many of our assumptions may not be valid at large t [e.g., the approximate forms of the signature factors, the replacement (5.15), etc.], we nevertheless find that the discrepancy is inherent in the model. The presence of the shoulder is due entirely to an anomalous bump in h_3 at $t = -0.3$ GeV^2. We can visualize this anomalous bump as follows. As we go away from the forward direction, the π-pole contribution $h_3^{(\pi)}$ grows rapidly until it reaches sufficient strength to destroy the cut contribution h_3^{cut} almost entirely. However, as t increases, $h_3^{(\pi)}$ falls off faster than h_3^{cut}, thus allowing h_3^{cut} to eventually regain its strength. As a consequence, a bump at $t = -0.3$ GeV^2 is present. We note that this effect does not depend on the particular model of the Regge cut. It depends only on the qualitative features of the cut.

TABLE I. A list of the cut "residue functions" for the pion-Pomeranchon amplitudes.

Amplitudes	Cut "residue functions" $\gamma_{ci}(\tau)$
h_1	$(1.57)\tau e^{-(2.24)\tau}$
h_2	0
h_3	$-(2.78\times 10^2)e^{-(2.21)\tau} - (7.0\times 10^2)\tau e^{-(2.96)\tau}$
h_4	$-(2.78\times 10^2)e^{-(2.21)\tau}$
h_5	$-(2.92)\tau^{1/2}e^{-(2.15)\tau}$

This discrepancy might be removed by including the contributions of the ρ pole and the A_2 pole, both of which contribute to h_4 but not h_3. Assuming strong exchange degeneracy, the combined ρ and A_2 contribution will have the following phase:

$$-\left(\frac{e^{-i\pi\alpha_\rho}-1}{\sin\pi\alpha_\rho}\right)+\left(\frac{e^{-i\pi\alpha_A}+1}{\sin\pi\alpha_A}\right)=\frac{2}{\sin\pi\alpha_\rho},$$

which is purely real and positive. The πP-cut contribution, on the other hand, is almost purely real negative. We therefore expect a destructive interference. Moreover, since the ρ and A_2 contributions are through tensor coupling, there is a factor $(-t)$ in their Regge residues. Hence the interference is substantial only at large values of t. In other words, while the amplitude h_3 acquires an anomalous bump, we expect h_4 to be substantially reduced in size, so that the combined effect can be a smooth cross section. This mechanism of interference between the cut amplitudes and the exchange-degenerate ρ and A_2 has been used earlier by Huang and Muzinich[23]; recently, Fox *et al.*[24] have suggested a similar mechanism in K^{*0} production.

A better understanding of this interference may be achieved by studying the reaction $np \to pn$

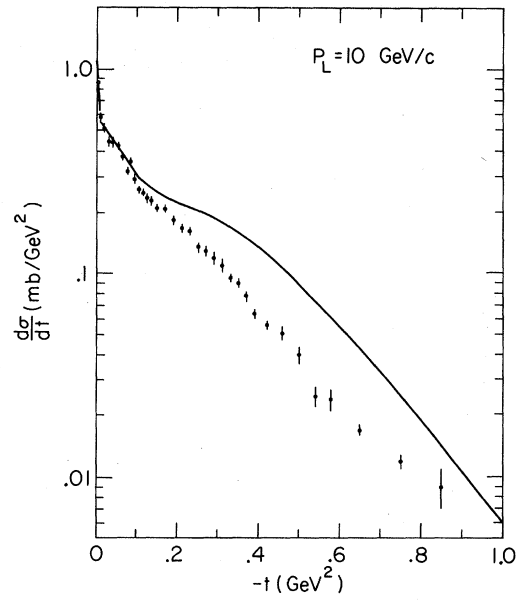

FIG. 6. Behavior of the model at larger t values, compared with the data of Ref. 3.

simultaneously with its line-reversed reaction $\bar{p}p \to \bar{n}n$. The contribution of ρ changes sign from $np \to pn$ to $\bar{p}p \to \bar{n}n$, whereas that of A_2 does not; the combined contribution therefore has the phase $e^{-i\pi\alpha_\rho(t)}$, which is almost 90° out of phase with the cut contribution. A prediction of such an interference would appear to be that the cross section for $\bar{p}p \to \bar{n}n$ is larger than that for $np \to pn$, which agrees qualitatively with the data,[25] with a shoulder at $t \simeq -0.3$ GeV^2.

The energy dependence of the forward cross section for the np charge-exchange reaction is found to obey the following power law:

$$\frac{d\sigma}{dt}(t=0) \sim p_L^{-2.33}.$$

The shape of the differential cross section however does not appear to change noticeably with energy, agreeing with experimental observations. A comparison of the energy dependence of the theoretical prediction with the data of Refs. 3 and 4 is shown in Fig. 7. The theoretical prediction appears to depend too steeply on energy. However, since the data contain a large systematic error, this apparent discrepancy may not be significant.

We do not predict a sizeable polarization, the predicted polarization being down by a factor of 10^{-4}. This is expected because the polarization is given in terms of πP-cut amplitudes alone, and all the cut amplitudes have approximately the same phase. To explain the observed polarization,[26] we must consider the contributions of other Regge poles.

We remark in passing that our model contains the essential features of the Reggeized absorption model of Henyey *et al.*[11] Like these authors we predict a flat, self-conspiratory cut that interferes destructively with the pion pole. We differ, however, in some particulars. Their model, because it assumes a helicity-conserving Pomeranchon, populates only h_3^{cut} and h_4^{cut}. The Mandelstam diagram model shows explicitly how h_1^{cut} and h_5^{cut} are suppressed. Our model also exhibits some other interesting features of the cut.[27]

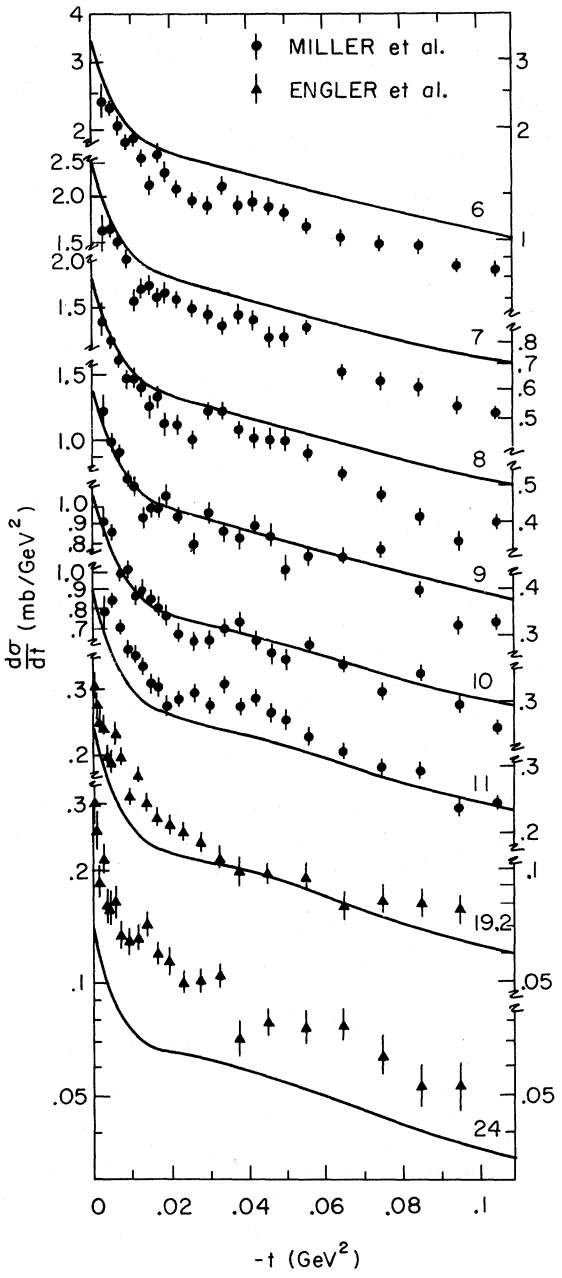

FIG. 7. Energy dependence of this model, compared with the data of Ref. 3 and Ref. 4.

VIII. CONCLUSION

We have developed a model in which the πP cut is calculated from the Mandelstam diagram. The πP cut is found to have the following properties: (i) It has even signature; (ii) it is self-conspiratory; (iii) it has a flat dependence on t; (iv) it interferes destructively with the π pole. Application is made to the np charge-exchange reaction. An excellent fit is obtained in the small-t region, but there is a significant discrepancy at large t values. This discrepancy can probably be removed in a more complicated model, by means of interference of cut amplitudes with the exchange-degenerate ρ and A_2.

ACKNOWLEDGMENTS

The author wishes to thank Professor L. M. Jones for her untiring guidance and constant encouragement throughout the course of this work.

APPENDIX

In the spinless case (e.g., 0^+0^- scattering), the cross structure function is given by

$$N=-s^2\,\frac{g_{1\sigma}g_{3\sigma}g_{31}\gamma_P}{4\pi}\int\frac{d^2k_1}{(2\pi)^2}\int_0^1 d\beta_1\beta_1{}^{\varphi_\pi}(1-\beta_1)^{\varphi_P}\int\frac{d\alpha_1}{2\pi}\int\frac{d(\alpha_1-\alpha)}{2\pi}\,\frac{1}{d_1d_2d_3d_4}\,, \tag{A1}$$

where

$$\begin{aligned}
d_1&=\alpha_1\beta_1 s-\vec{k}_1{}^2-m_1{}^2+i\epsilon,\\
d_2&=(\alpha_1-\alpha)\beta_1 s-(\vec{k}_1-\vec{k})^2-m_3{}^2+i\epsilon,\\
d_3&=\left(\alpha_1-\frac{m^2}{s}\right)(\beta_1-1)s-\vec{k}_1{}^2-m_\sigma{}^2+i\epsilon,\\
d_4&=\left(\alpha_1-\alpha-\frac{m_3{}^2+\tau}{s}\right)(\beta_1-1)s-(\vec{k}_1-\vec{k}+\vec{q})^2-m_\sigma{}^2+i\epsilon.
\end{aligned} \tag{A2}$$

We note that the integrands appearing in

$$\int\frac{d\alpha_1}{2\pi}\,\frac{1}{d_1d_3}\ \text{and}\ \int\frac{d(\alpha_1-\alpha)}{2\pi}\,\frac{1}{d_2d_4}$$

have the right behavior at infinity to make the integrals convergent. The presence of spin, however, introduces extra numerators into the integrand of (A1). These numerators, in general, contain the internal momenta, the presence of which introduces divergence in (A1). Since we are considering only π-exchange reactions, we will encounter one of the following pairs of particles at the cross: (1) NN, (ii) $N\Delta$, (iii) $\pi\rho$, and (iv) πf. In general, (A1) is modified by the presence of spin to be

$$N_{\lambda_3\lambda_1}=-s^2\,\frac{g_{1\sigma}g_{3\sigma}\gamma_P}{4\pi}\int\frac{d^2k}{(2\pi)^2}\int_0^1 d\beta_1\beta_1{}^{\varphi_\pi}(1-\beta_1)^{\varphi_P}\int\frac{d\alpha_1}{2\pi}\int\frac{d(\alpha_1-\alpha)}{2\pi}\,\frac{B_{\lambda_3\lambda_1}G_{31}}{d_1d_2d_3d_4}\,. \tag{A3}$$

A collection of $B_{\lambda_3\lambda_1}$ for the four types of crosses is shown in Table II. The fact that $B_{\lambda_3\lambda_1}$ involves the internal momenta has the consequence that the α_1 and $(\alpha_1-\alpha)$ integrals will be divergent. To overcome this divergence, we must introduce softening factors in the form factors G_{31}. This can simply be achieved by putting

$$\begin{aligned}
G_{31}&=\left(\frac{m_3{}^2-\Lambda_3{}^2}{k_3{}^2-\Lambda_3{}^2+i\epsilon}\right)^{n_3}\left(\frac{m_1{}^2-\Lambda_1{}^2}{k_1{}^2-\Lambda_1{}^2+i\epsilon}\right)^{n_1}\\
&=\left(\frac{m_3{}^2-\Lambda_3{}^2}{(\alpha_1-\alpha)\beta_1 s-(\vec{k}_1-\vec{k})^2-\Lambda_3{}^2+i\epsilon}\right)^{n_3}\left(\frac{m_1{}^2-\Lambda_1{}^2}{\alpha_1\beta_1 s-\vec{k}_1{}^2-\Lambda_1{}^2+i\epsilon}\right)^{n_1},
\end{aligned}$$

where the integers n_3 and n_1 are the minimal multiplicities.

In general, n_3 and n_1 depend on both the spins of the external particles and the coupling at the Regge vertex. Since the propagator of a particle of spin s contains a numerator which is a function of the internal momentum to $2s$ degree, it follows that the propagator itself requires $2s$ multiplicity. The effect of the coupling at the Regge vertex is more complicated, and we shall consider each case separately. The details are complex, but the reasoning is straightforward. We expand the function $B_{\lambda_3\lambda_1}$ in terms of

TABLE II. List of the cross numerator functions $B_{\lambda_3\lambda_1}$ together with corresponding minimal multiplicities n_3 and n_1.

Cross	n_3	n_1	$B_{\lambda_3\lambda_1}$
NN	1	1	$\bar{u}_{\lambda_3}(\not{k}_1-\not{k}+m)\gamma_5(\not{k}_1+m)u_{\lambda_1}$
$N\Delta$	3	2	$\bar{\Delta}^\mu_{\lambda_3}(\not{k}_1-\not{k}+m_\Delta)\left(-g_{\mu\nu}+\frac{1}{3}\gamma_\mu\gamma_\nu+\frac{2(k_1-k)_\mu(k_1-k)_\nu}{3m_\Delta{}^2}-\frac{(k_1-k)_\mu\gamma_\nu-(k_1-k)_\nu\gamma_\mu}{3m_\Delta}\right)k^\nu(\not{k}_1+m)u_{\lambda_1}$
$\pi\rho$	1	1	$\epsilon^{\dagger\mu}_{\lambda_3}\left(-g_{\mu\nu}+\frac{(k_1-k)_\mu(k_1-k)_\nu}{m_\rho{}^2}\right)(k_1+k)^\nu$
πf	4	2	$f^{\dagger\mu\nu}_{\lambda_3}\left(\frac{1}{2}P_{\mu\rho}P_{\nu\sigma}+\frac{1}{2}P_{\mu\sigma}P_{\nu\rho}-\frac{1}{3}P_{\mu\nu}P_{\rho\sigma}\right)k_1^\rho k^\sigma$, where $P_{\mu\nu}=-g_{\mu\nu}+\frac{(k_1-k)_\mu(k_1-k)_\nu}{m_f{}^2}$

the internal momenta, k and k_1, explicitly for each case. We next express these functions in terms of the variables of (4.3), and look at the factor with the highest powers in α_1 and $\alpha_1 - \alpha$. For each power of α_1 in $B_{\lambda_3\lambda_1}$ we assign a value of one to n_1, and for each power of $\alpha_1 - \alpha$ in $B_{\lambda_3\lambda_1}$ we assign a value of one to n_3. The result of such an assignment is given in Table II.

*Work supported in part by the National Science Foundation under Grant No. NSF GP 25303.

[1]H. Palevsky *et al.*, Phys. Rev. Letters 9, 509 (1962).
[2]G. Manning *et al.*, Nuovo Cimento 41A, 167 (1966).
[3]E. L. Miller *et al.*, Phys. Rev. Letters 26, 984 (1971).
[4]J. Engler *et al.*, Phys. Letters 34B, 528 (1971).
[5]R. J. N. Phillips, Nucl. Phys. B2, 394 (1967).
[6]F. Arbab and J. W. Dash, Phys. Rev. 163, 1603 (1967).
[7]J. Ball, W. Frazer, and M. Jacob, Phys. Rev. Letters 20, 518 (1968).
[8]M. LeBellac, Phys. Letters 25B, 524 (1967).
[9]M. Aderholz *et al.*, Phys. Letters 27B, 174 (1968).
[10]J. A. Gaidos *et al.*, Phys. Rev. D 1, 3190 (1970).
[11]F. Henyey, G. L. Kane, J. Pumplin, and M. H. Ross, Phys. Rev. 182, 1579 (1969).
[12]A. P. Contogouris and J. P. Lebrun, Nuovo Cimento 64A, 627 (1969).
[13]A. B. Kaidalov and B. M. Karnakov, Phys. Letters 29B, 372 (1969).
[14]G. L. Kane *et al.*, Phys. Rev. Letters 25, 1519 (1970).
[15]S. Mandelstam, Nuovo Cimento 30, 1148 (1963).
[16]J. C. Polkinghorne, J. Math. Phys. 4, 1396 (1963).
[17]H. Rothe, Phys. Rev. 159, 1471 (1967).
[18]V. N. Gribov, Zh. Eksp. Teor. Fiz. 53, 654 (1968) [Sov. Phys. JETP 26, 414 (1968)]. The technique used in extracting the high-energy behavior in this paper is closely related to the work of Shau-Jin Chang and Shang-Keng Ma, Phys. Rev. 188, 2385 (1969).
[19]S. Frautschi and L. Jones, Phys. Rev. 164, 1918 (1967).
[20]G. G. Beznogikh *et al.*, Phys. Letters 30B, 274 (1969).
[21]Letting $\Lambda^2 \to \infty$ may appear miraculous when it is needed in the beginning to ensure the convergence of the loop integral. A detailed calculation, however, reveals that in taking Λ^2 to ∞, we are merely shifting the divergence to the upper end point in the β_1 integral, as we introduce an extra factor of $(1-\beta)^{-1}$. The end-point divergence of the β_1 integral and the necessary assumption made in order to obtain a finite result are discussed in Sec. V.
[22]D. Branson, Phys. Rev. 179, 1608 (1969).
[23]K. Huang and I. J. Muzinich, Phys. Rev. 164, 1726 (1967).
[24]G. C. Fox *et al.*, Phys. Rev. D 4, 2647 (1971).
[25]W. Beusch *et al.*, paper submitted to the Fifteenth International Conference on High-Energy Physics, Kiev, U.S.S.R., 1970 (unpublished).
[26]P. R. Robrish *et al.*, Phys. Letters 31B, 617 (1970).
[27]Application of the model to $\pi N \to \rho N$ and $\pi N \to \rho \Delta$ is presently being carried out; results will be reported in another paper.

PHYSICAL REVIEW D VOLUME 5, NUMBER 9 1 MAY 1972

Infinite-Component Wave Equations and Mass Splittings Within SU(3) and SU(2) Multiplets*

A. O. Barut and William Brink Monsma†
Institute for Theoretical Physics, Department of Physics and Astrophysics, University of Colorado, Boulder, Colorado 80302
(Received 6 July 1971)

Earlier work describing baryon excited states by the group O(4,2) is extended with particular emphasis on the SU(3) properties. A single irreducible representation of O(4,2) $\times$ SU(3) $\times$ SU(3) is used. The postulates of the theory of infinite-component wave equations are contrasted and compared with those leading to the Okubo and isospin mass-splitting formulas. Tables and curves are presented for mass formulas, mass splittings, and magnetic moments, which are in agreement with experiment.

I. INTRODUCTION

In the usual mass formula based on SU(3) symmetry, one postulates that m or m^2 is a particular combination of tensor operators with respect to SU(3) representations.[1] On the other hand, the covariant wave equation from which the mass spectrum is derived is written in terms of the components of p^μ and some algebraic operators Γ^μ, and from this one evaluates the eigenvalues of the